

# Analysis of a vibration isolation table comprising post-buckled $\Gamma$ -shaped beam isolators

T. Sasaki<sup>1</sup> and T.P. Waters<sup>2</sup>

<sup>1</sup> Associate Professor, University of Kitakyushu, Japan

<sup>2</sup> Associate Professor, University of Southampton, UK

E-mail: sasa@kitakyu-u.ac.jp

**Abstract.** In this paper, the static and dynamic characteristics of a nonlinear passive vibration isolation table is investigated through finite element analysis. The intended application is specifically isolation in the vertical direction where the isolator is required to be sufficiently stiff statically to bear the weight of the isolated object and soft dynamically for small oscillations about its equilibrium position. The modelled configuration consists of a rigid isolation table mounted on two  $\Gamma$ -shaped beam isolators which are loaded to their post-buckled state in their unstable buckling mode by the weight of the isolated mass. A nonlinear static analysis is presented to establish the negative stiffness provided by the buckled beams, and two linear springs are then added in parallel which are chosen to have just sufficient stiffness to restore stability. Modal analysis of the linearized system about its statically deformed position (1mm) gives a natural frequency of just 1Hz which is considerably lower than is achievable by a linear isolator. Motion transmissibility of the linearized system shows a non-resonant isolation region spanning two decades when the system is perfectly symmetric but additional resonance peaks appear when asymmetries are included in either the mass or stiffness distribution. Several strategies are explored for reducing the prominence of these resonances.

## 1. Introduction

Passive isolators remain the most commonly adopted form of isolator due to their simplicity, stability and low cost. A key trade-off in the selection of most passive mounts is their static load bearing capacity, which requires high stiffness, versus their isolation bandwidth which requires low stiffness. This intrinsic compromise, which is a consequence of their approximately linear elastic behaviour, can be circumvented by designing a softening nonlinearity into the force-deflection curve. Ideally, the mount is stiff when loaded statically up to its intended equilibrium position, about which it has a low stiffness to small dynamic perturbations. Many nonlinear spring mechanisms have been proposed, especially over the last 15 years. An extensive review is presented by Ibrahim [1]. Mechanisms studied are often geometrically [2] or magnetically nonlinear [3] but buckled elements are perhaps the most common experimental manifestations, as in [4] for example. However, such mechanisms can require cumbersome arrangements particularly in order to constrain lateral motions. To overcome these problems, the authors have previously proposed a  $\Gamma$ -shaped (inverted L-shaped) beam isolator which offers a potentially simple and compact realisation. Analytical and experimental characterisation of the isolator has been reported in previous papers [5], [6]. This isolator exhibited improved isolation performance compared to an equivalent linear passive isolator but the system is unrepresentative of practical cases where multiple isolators are required to support a distributed mass.

This paper considers a vibration isolation table which is supported by a pair of post-buckled  $\Gamma$ -shaped beam isolators. This model accounts for the moment of inertia of the isolation table and the rotational stiffness provided by the spacing of the beam springs. The configuration is described in section 2. In section 3 finite element results are presented for the nonlinear static analysis of the system, followed by modal and harmonic base excitation analyses of the system when linearized about its equilibrium position. Perturbations are introduced to the mass and stiffness distributions in section 4 to illustrate the sensitivity of the system to asymmetry. Also, section 4 identifies the source of this sensitivity which can be mitigated by detuning the system from near quasi-zero stiffness (QZS).

## 2. A vibration table comprising post-buckled $\Gamma$ -shaped beam isolators

A schematic of a passive nonlinear vibration isolation table is shown in Fig. 1. The key feature of the arrangement are the  $\Gamma$ -shaped beams. These can be made to buckle in their stable buckling mode so as to provide low stiffness to dynamic perturbations about an equilibrium position whilst providing high static stiffness to support the weight of the isolated object. Here, however, the beams are made to buckle in their unstable buckling mode in order to provide negative stiffness to counteract the positive stiffness of a pair of linear springs. A rigid isolation table is suspended from the vertices of the  $\Gamma$ -shaped beams by short wires to facilitate hinged joints. An isolated object can be placed at the centre of the isolation table. By tuning the spring constant and the initial extension of the linear springs, Quasi-Zero-Stiffness (QZS) can be realized for an isolated object with arbitrary mass.

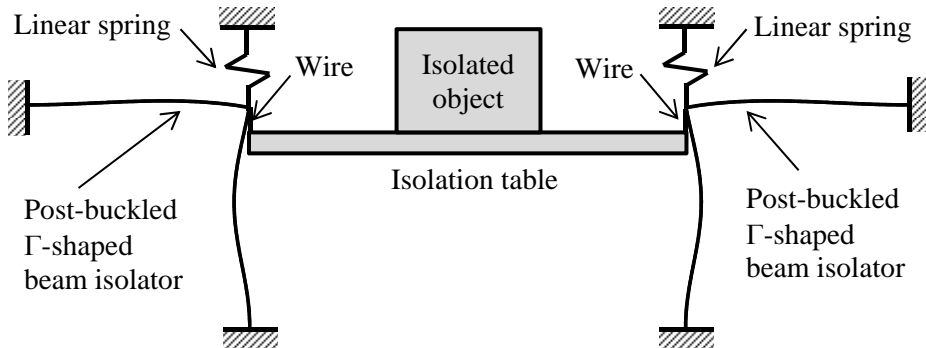


Fig.1. Schematic of a passive vibration isolation system comprising post-buckled  $\Gamma$ -shaped beam isolators

## 3. Static and dynamic behaviour of the isolation table

In this section, the static and dynamic behaviour of the proposed isolation system is predicted using Finite Element analysis. The parameter values of the model are listed in Table 1. The dimensions of the  $\Gamma$ -shaped beams were chosen to be the same as used in previously published numerical and experimental studies [5],[6].

### 3.1. Static behaviour

Fig. 2 shows the force-deflection curve in the vertical direction when a downward displacement is imposed at the centre of the isolation table such that the  $\Gamma$ -shaped beams buckle in their unstable buckling mode. In this analysis, the linear springs and gravitational acceleration are omitted. Motion of the isolation table is purely in the vertical direction owing to symmetry of the system. The solid line in Fig. 2 shows the static restoring force and the dashed line shows the tangent stiffness, i.e. the gradient of the force-deflection curve. From the figure, it is confirmed that the system exhibits negative stiffness in its post-buckled state. However, the system can be stabilised by the addition of linear springs of appropriate stiffness to yield arbitrarily low overall tangent stiffness.

Table 1. Dimensions of the  $\Gamma$ -shaped beam isolators and the isolation table

$\Gamma$ -shaped beam isolators	Vertical beam	Length [mm]	100
		Width [mm]	18
		Thickness [mm]	0.5
	Horizontal beam	Length [mm]	100
		Width [mm]	18
		Thickness [mm]	0.7
Isolation table		Length [mm]	300
		Width [mm]	50
		Thickness [mm]	50
Wire (circular cross-section)		Length [mm]	10
		Radius [mm]	1.5
Common material parameters		Young's modulus [GPa]	180.36
		Poisson's ratio [-]	0.3
		Density [ $\text{kg}/\text{m}^3$ ]	7000

A static equilibrium position of about 1mm was chosen to allow for modest dynamic oscillations within the post-buckled state. At this position, the tangent stiffness is about  $-5,500\text{N}/\text{m}$ . The linear springs were chosen to have a stiffness of  $3000\text{N}/\text{m}$  to ensure low but positive stiffness of the system. The parameter values for the system are listed in Table 2.

When gravitational acceleration was included in the model the isolators buckled under the weight of the isolated mass and the isolation table reached a stable equilibrium position at about 1mm below its unloaded state, as expected from the preceding static analysis. The linearized stiffness matrix in its post-buckled state was then used to conduct subsequent modal analysis and base excited harmonic analysis.

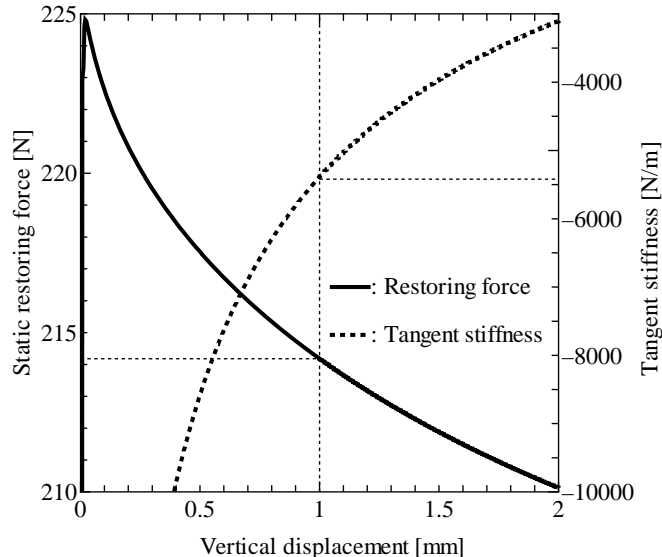


Fig. 2 Static force and tangent stiffness as functions of applied vertical displacement for the system without stabilizing linear springs

Table 2. Specification of the linear spring and mass of the isolated object

Linear spring	Spring constant [N/m]	3000
	Initial tension [N]	0.15
Isolated object	Mass [kg]	17.24
	Moment of inertia [ $\text{kg} \cdot \text{m}^2$ ]	0

### 3.2. Modal analysis in the post-buckled state

Modal analysis was conducted using the linearized stiffness matrix in the static equilibrium state. At this stage, the acceleration of gravity was omitted so that the pendulum mode of the isolation table was not obtained. The natural frequencies of the first ten modes are listed in Table 3. The fundamental natural frequency of the system is about 1Hz. By comparison, a linear single degree-of-freedom system with the same static deflection would result in a natural frequency of over 15Hz. The mode shapes of the first 10 modes are shown in Fig. 3. The black and red lines correspond to the static deformation shape and the mode shape respectively. From Table 3, it is seen that there are three additional modes at slightly higher frequencies than the fundamental mode that could jeopardise the system's low frequency isolation performance. However, by inspection of Fig. 3(b) to (d) it is apparent that the centre of the isolation table, where an isolated object is located, corresponds to a nodal point of these additional modes and so they are not expected to transmit vertical motion.

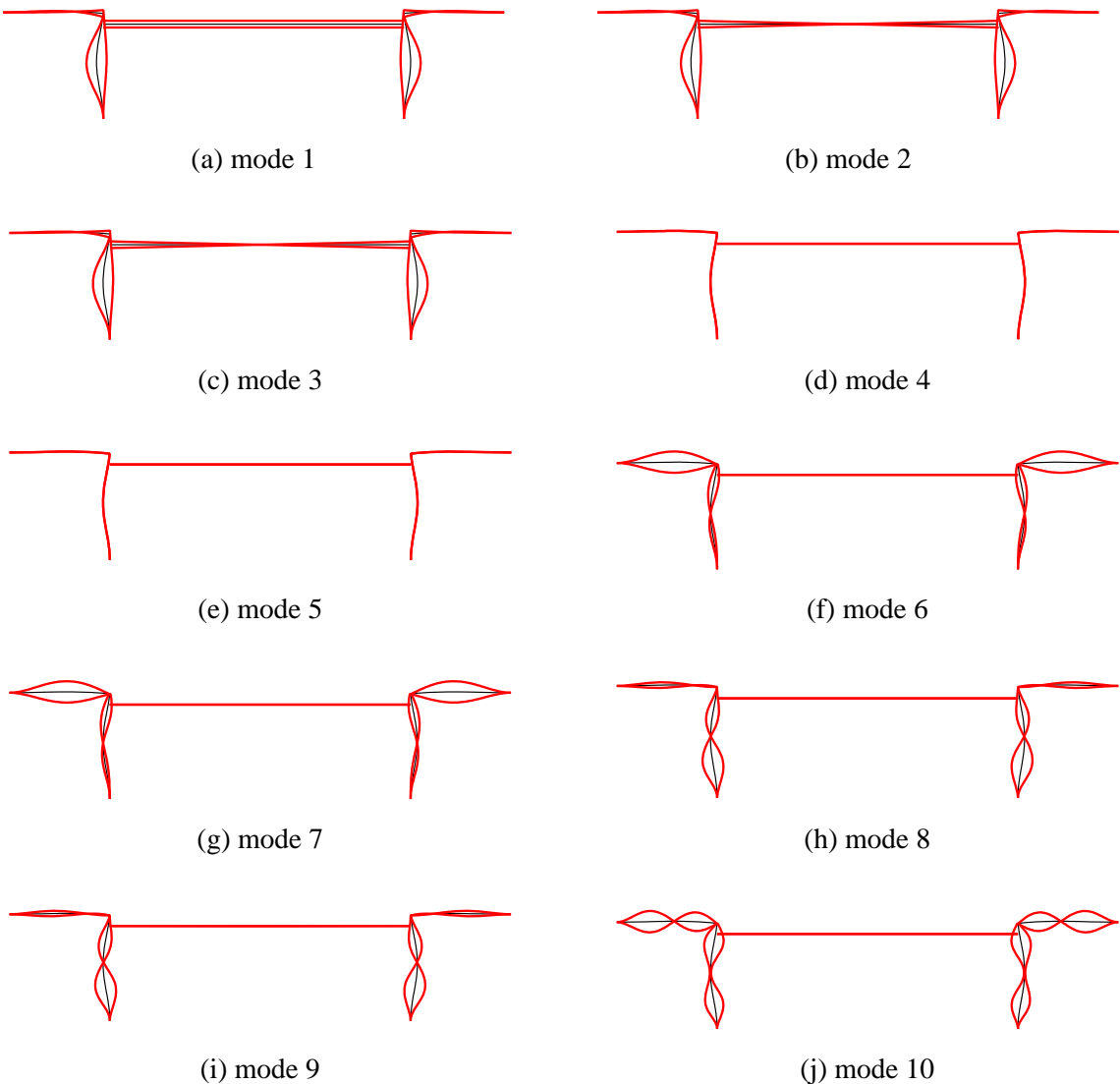


Fig. 3. Mode shapes of linearized model about an equilibrium position of 1mm  
 (— static deformation, — mode shape)

Table 3. Natural frequencies of the post-buckled system

Order	Natural frequency [Hz]	Order	Natural frequency [Hz]
1	1.02	6	266
2	3.16	7	266
3	5.23	8	495
4	6.44 (out-of-plane)	9	496
5	52.7 (out-of-plane)	10	785

### 3.3. Motion transmissibility in the post-buckled state

Harmonic base excitation of the model in its post-buckled state was applied to all six mounting points shown in Fig. 1 and a linear harmonic analysis was conducted based on modal superposition of the first 30 modes. The motion transmissibility between the base and the isolated object is shown by the black line in Fig. 4. From the figure, it is confirmed that the first resonance peak appears at the first natural frequency and the next resonance appears at the sixth natural frequency. As anticipated from inspection of the mode shapes, the intervening modes are neither excited nor observed in the frequency response which permits good isolation performance in this frequency range. By comparison, the frequency response of an equivalent linear single degree-of-freedom system is shown by the blue dashed line in Fig. 4. The proposed system is seen to offer substantially improved isolation performance from 2-200Hz.

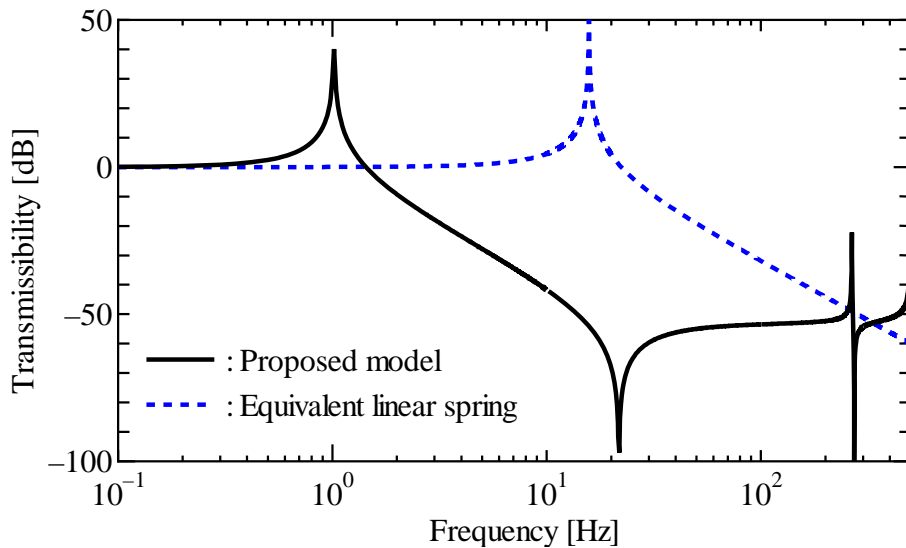


Fig. 4. Motion transmissibility of the linearized model about an equilibrium position of 1mm compared with a linear single degree-of-freedom system with the same static deflection

### 4. Investigation of the effects of asymmetry on isolation performance

The isolation performance suggested by Fig. 4 can only be realized when symmetry of the system is assured. In practice, asymmetry is inevitable due to manufacturing variability and imprecise installation. In this section, the effects of both stiffness and mass asymmetry are investigated. In both cases the elastic centre can be expected to deviate from the centre of mass thereby coupling translational and rotational degrees of freedom.

#### 4.1. Frequency response of asymmetric system

Asymmetric stiffness was introduced by perturbing the spring constant of the right linear spring whilst leaving the stiffness of the left spring unchanged. Fig. 5(a) to (c) show the results for stiffness changes of  $\pm 3\%$  and  $-20\%$ . It is seen that the second and third modes, which did not appear when the system was symmetric, are now apparent owing to small shifts in their nodal points. These peaks disrupt an otherwise broad isolation region.

Mass asymmetry was introduced by shifting the position of the isolated mass by 0.2mm from the centre of the isolation table. The predicted motion transmissibility is shown in Fig. 5(d). Again, the second and the third modes are prominent in the response and are detrimental to the isolation performance. However, in this case the fundamental resonance has reduced to less than 0.2Hz. The system is now close to quasi-zero stiffness since the shift in weight distribution has altered the tangent stiffnesses of the buckled beams. In practice, such a marginally stable system may be undesirable and a very low natural frequency may render the system too responsive to any direct forcing of the isolated object.

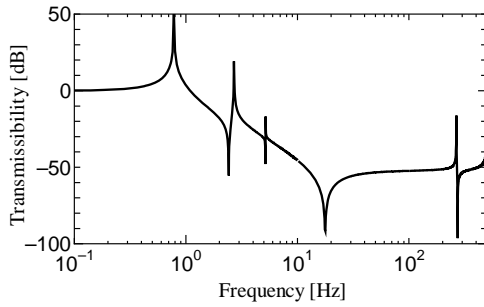


Fig. 5(a) Transmissibility of system with asymmetric stiffness (spring constant perturbed by  $+3\%$  to 3090N/m)

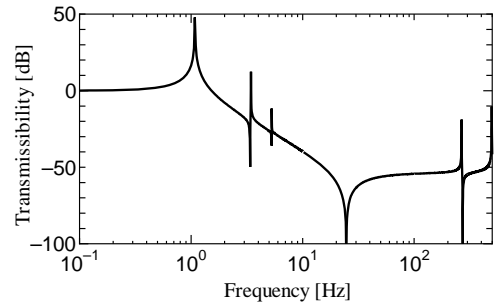


Fig. 5(b) Transmissibility of system with asymmetric stiffness (spring constant perturbed by  $-3\%$  to 2910N/m)

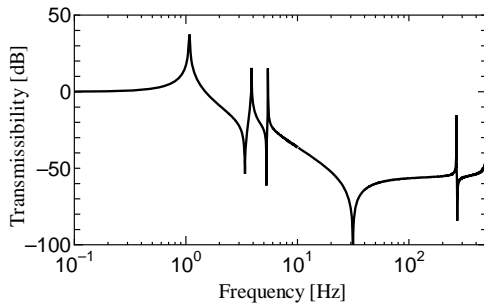


Fig. 5(c) Transmissibility of system with asymmetric stiffness (spring constant perturbed by  $-20\%$  to 2400N/m)

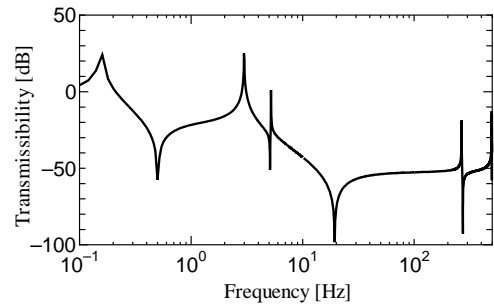


Fig. 5(d) Transmissibility of system with asymmetric mass distribution (isolated object shifted by 0.2mm from the centre of the isolation table)

#### 4.2. Mitigation of additional resonances due to asymmetry

In the previous section, it is shown that the isolation performance of proposed system can deteriorate significantly owing to small asymmetries of the system. In this section, two possible countermeasures for mitigating the effect of asymmetry on the isolation performance are investigated.

**4.2.1. Effect of isolation table** The second and the third natural modes are dominated by rotational motion of the isolation table, as shown in Fig. 3(b) and 3(c), and are expected to be sensitive to the moment of inertia of the isolation table. This parameter was varied in the model by increasing its length from 300mm to 900mm, and also reducing its length to 100mm. The mass of the isolated

object was also adjusted so that the overall mass of the isolated object and the isolation table was unchanged. Figs. 6 and Figs. 7 show the frequency responses for the 900mm model and the 100mm model respectively. Each model was considered with and without stiffness asymmetry. Comparison of Figs. 6 and 7 with Fig. 5(a-b) suggests that the length of the isolation table does not assist greatly in mitigating the system's sensitivity to asymmetry.

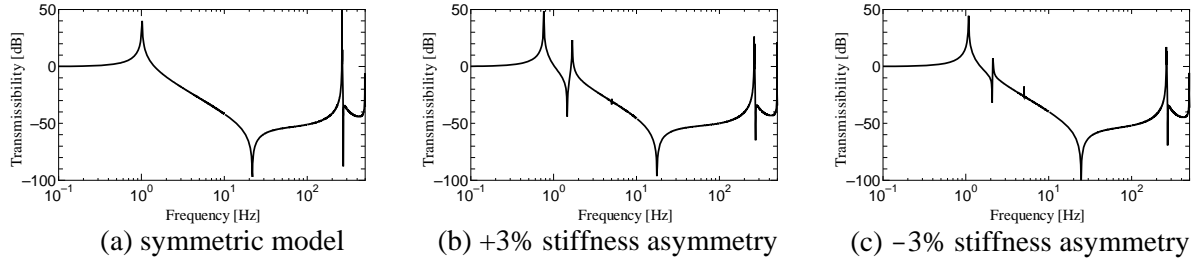


Fig. 6. Motion transmissibility of system with lengthened (900mm) isolation table

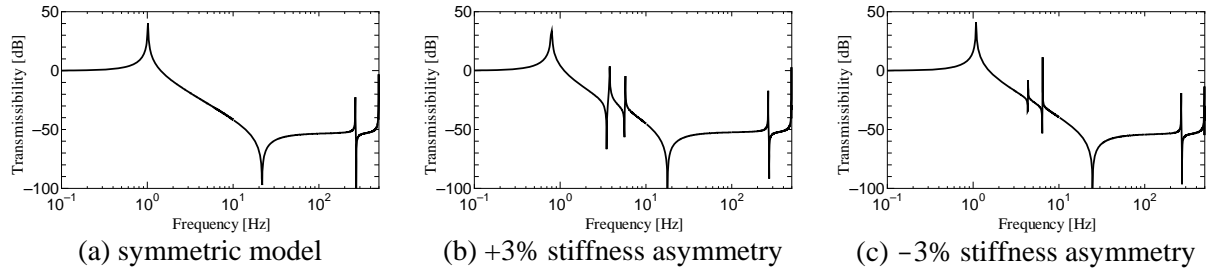


Fig. 7. Motion transmissibility of system with shortened (100mm) isolation table

**4.2.2. Effect of static deflection in post-buckled state** The static deflection of the system was increased from 1mm to 2mm by adjusting the pretension of the linear springs. Figs. 8(a) to 8(c) show the motion transmissibility of the system with and without asymmetry in the linear springs. The prominence of the second and third modes is reduced considerably. By lowering the static equilibrium position further into the buckled region the combined negative stiffness of the buckled springs has almost halved from -5,500N/m to about -3000N/m, according to Fig. 2, such that the overall stiffness with the linear springs installed increases substantially from about 500N/m to 3000N/m. Any subsequent asymmetry in one of the linear springs no longer has a disproportionate effect on the stiffness distribution and hence the position of the elastic centre is less affected. The cost of this benefit is roughly to double the fundamental natural frequency. Figs. 8(d) and 8(e) show the corresponding results for an asymmetric mass distribution in which the isolated mass is shifted first by 0.2mm and then by 1.0mm, thereby shifting the centre of mass away from the elastic centre. Again, the system is seen to be less sensitive to mass asymmetry than when the equilibrium position was set to 1mm. Fig. 8(f) shows the result for the same system as in Fig. 8(e) but with a constant damping ratio of 0.5% included in the model which lessens the severity of the offending resonances.

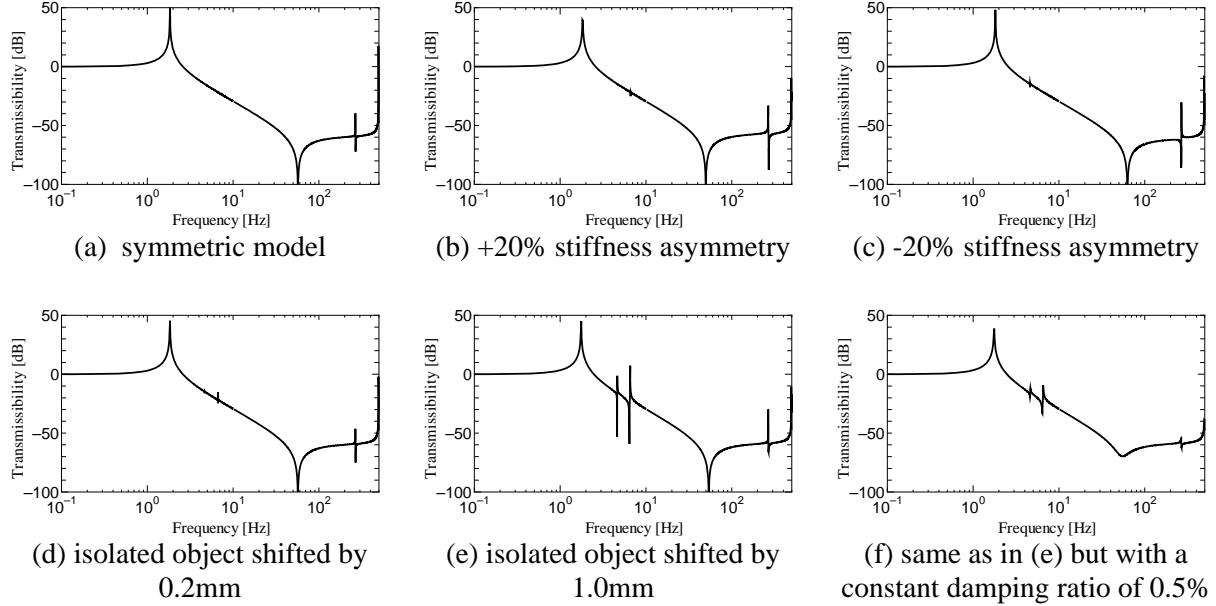


Fig. 8. Motion transmissibility of linearized model about an equilibrium position of 2mm

## 5. Conclusions

This paper has investigated, by Finite Element analysis, the static and dynamic characteristics of a vibration isolation table comprising post-buckled  $\Gamma$ -shaped beam isolators. The fundamental resonance of the proposed system occurs at about 1Hz for a static deflection of just 1mm, as compared to 15Hz for a linear isolator with the same static deflection. If symmetry is assured then the system is free from other resonances until above 200Hz. However, small asymmetries in either the stiffness or mass distribution cause intervening resonances to be excited thus disrupting the wide isolation region. The system is found to be significantly less sensitive to asymmetries if the beam isolators are used further into their post-buckled region, although this has the undesirable side-effect of increasing the fundamental natural frequency.

## References

- [1] Ibrahim, R. A., (2008), Recent Advances in Nonlinear Passive Vibration Isolators, *Journal of Sound and Vibration*, 314, pp. 371-452.
- [2] Park, S. T. and Luu, T. T., (2007), Techniques for Optimizing Parameters of Negative Stiffness, *Proc of IMechE, Journal of Mechanical Engineering Science*, Vol. 221, pp. 505-511.
- [3] Robertson, W.S.P., (2013), Modelling and design of magnetic levitation systems for vibration isolation, PhD thesis, University of Adelaide.
- [4] Winterflood, J., Blair, D. G. and Slagmolen, B., (2002), High Performance Vibration Isolation using Springs in Euler Column Buckling Mode, *Physics Letters A*, Vol. 300, pp. 122-130.
- [5] Sasaki, T., Waters, T.P. and Tsuji, Y., (2015), Experimental study on a nonlinear vibration isolator based on a post-buckled inverted L-shaped beam, *Mechanical Engineering Journal* Vol.2, No.3.
- [6] Tsuji, Y., Sasaki, T., Waters, T.P., Fujito, K. and Wang, D., (2014), A Nonlinear Vibration Isolator Based on a Post-buckled Inverted L-shaped Beam, *The 6th World Conference on Structural Control and Monitoring*, Barcelona.